Optically coupled electrical sampling system with 4-GHz bandwidth

S. B. Samaan

Tektronix Inc., M/S 50-276, P. O. Box 500, Beaverton, Oregon 97077

L. Wilson Pearson

McDonnell Douglas Research Laboratories, P. O. Box 516, Saint Louis, Missouri 63166

Charles E. Smith

Electrical Engineering Department, University of Mississippi, University, Mississippi 38677

(Received 6 August 1986; accepted for publication 5 October 1986)

A new approach to the design of a fiber-optic interface that links a commercial sampling head to its matching time-domain reflectometer (TDR)/sampler oscilloscope plug-in unit is reported. Three fiber-optic links replace the wired signal paths of the original design that convey the vertical error signal, the feedback signal, and the horizontal sampling command signal between the sampling head and the oscilloscope sampling plug-in. The dielectric fiber pigtails allow the use of the sampling head inside objects that need to be electromagnetically insulated from the instrumentation system. Low-frequency analog links are used to convey the error and feedback signals. The sampling command signal is conveyed via a link where a powerful, fast-rise infrared laser pulse is generated. The laser pulse is used to trigger an avalanche transistor in the strobe generator circuit of the sampling head by directly coupling the optical energy to the transistor chip. This direct method of detection minimizes the time jitter introduced to the strobe signal, resulting in a bandwidth of 4 GHz. Some of the results of the tests which were carried out on the system are reported.

INTRODUCTION

In some electromagnetic scattering measurements, it is necessary to probe the time-domain currents induced on the surface of a metallic scatterer as a result of an impinging high-frequency electromagnetic field. For such a measurement, a surface-current probe[1] may be used in conjunction with a sampling head that can be placed inside the scatterer if it is a closed object. High-frequency sampling systems are a convenient means of observing repetitive waveforms with a frequency content in excess of 1 GHz. Conventional systems consist of a sampling head that may be connected via an extension cable to a mainframe oscilloscope sampling plug-in unit. In a scattering measurement, the extension cable causes a disturbance of the incident and scattered electromagnetic (EM) fields; such a disturbance cannot always be controlled through geometrical rearrangement. Also, the high-frequency EM fields may induce noise voltages in the extension cable, thus rendering the measurement results useless. To solve these problems, Holbrook and Dyer[2-4] constructed an optically coupled sampling system in which the error, feedback, and sampling command signals (usually carried by the extension cable) were conveyed over fiber-optic pigtails using three fiber-optic links. By replacing the metallic cables with the very thin dielectric fiber pigtails, the problems of field disturbance and electromagnetic interference could be essentially eliminated.

The system constructed by Holbrook and Dyer utilizes the Tektronix S-6 sampling head in conjunction with the 7S12 time-domain reflectometer (TDR)/sampler unit. Holbrook and Dyer used two low-frequency analog fiber-optic links to deliver the error and feedback signals. The sampling command signal in the Holbrook–Dyer system was delivered from the sampling plug-in unit via a laser pulse generated by a fast, low-power, cw laser diode, and was detected at the sampling head with an avalanche photodiode. The output of the photodiode was used to drive an avalanche buffer stage that, in turn, triggered the avalanche transistor in the S-6 strobe generator circuit.[5] The Holbrook–Dyer system manifested a nominal bandwidth of 1 GHz, with a maximum of 2 GHz under ideal conditions. The bandwidth was limited mainly by the time jitter introduced to the sampling command signal.

Lawton and Andrews[6-8] have patented a dual-mode system for sampling fast electrical or optical signals. In that system, the sampling gate, which is built around two GaAs photoconductors, is strobed with narrow optical pulses to acquire an electrical waveform. In the Lawton–Andrews system, the error and feedback signals are transmitted using hardwired links. If, however, those signals along with the optical strobe are coupled using fiber-optic pigtails, a system which performs a function similar to the function of the one presented here could perhaps be realized.

The present work adopts the Holbrook configuration in an effort to obtain improved performance. This configuration has the potential for a large bandwidth.

I. SAMPLING OSCILLOSCOPE OPERATION

This section provides a brief overview of the relevant functional aspects of the sampling system used. This information is detailed elsewhere,[5,9,10] and is synopsized here for the sake of completeness. A simplified block diagram that complements the following discussion is shown in Fig. 1.

 0034-6748/87/010060-09$01.30

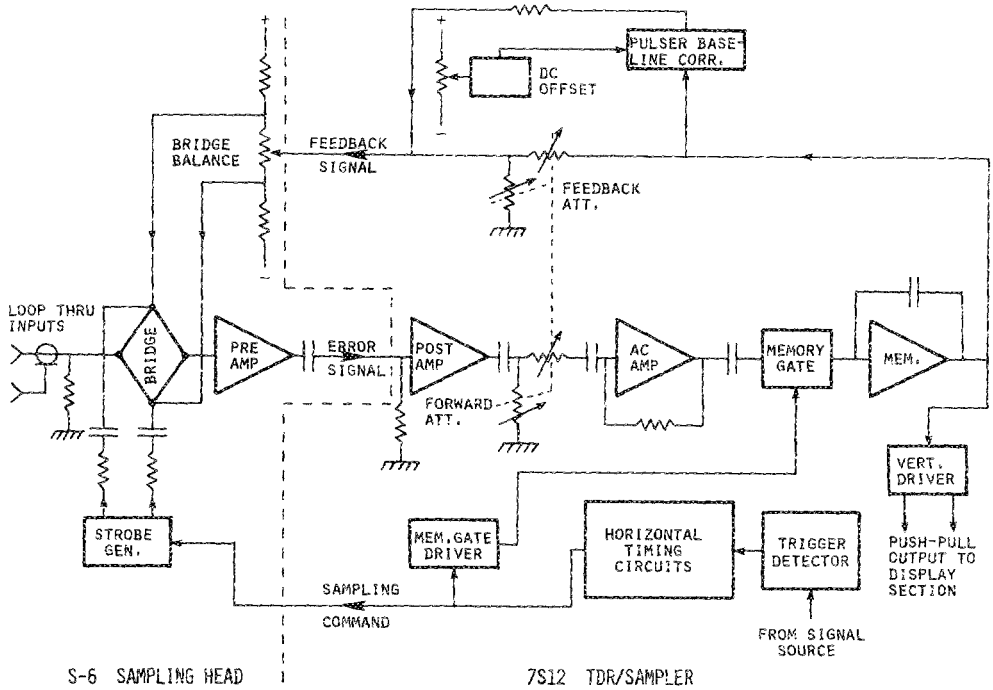

FIG. 1. Simplified block diagram of the S-6/7S12 sampling system used.

A key element of the sampling head is a high-speed diode sampling bridge that is used to capture samples of the observed signal. The bridge circuit is followed by a preamplifier with a slightly capacitive input, which serves to stretch the sample signal in time and thus reduces its bandwidth considerably. The sampling bridge is controlled by a strobe generator which, upon receiving a command from the mainframe sampler plug-in, produces very narrow (subnanosecond) strobe pulses to open the sampling gate. The sampler plug-in contains the horizontal timing circuits that generate the sampling command signal, which determines when a sample is to be taken. Samples are acquired sequentially in time with respect to a time reference (trigger) point on the observed signal. The sampling plug-in also contains vertical amplifiers which make the acquired samples available for the oscilloscope display section. The value of a sample is communicated between the sampling head and the mainframe sampler using a so-called error signal scheme. The mainframe sampler retains in an analog memory the value of the last sample and sends it to the sampling head over a "feedback" line . When the sampling head acquires a new sample, it sends to the mainframe sampler the difference "error" between the value of this sample and the last one. This error updates the output of the analog memory circuit (and also the display) after passing through a gate at the memory input. The memory gate is an analog gate which is opened only for a brief time duration to capture the transient error signal. The acquired samples are displayed on the screen in the proper temporal order for a coherent reproduction of the high-frequency signal.

II. DESIGN OF THE FIBER-OPTIC LINKS

In order to successfully replace the conductors indicated in Fig. 1 with optical fibers, the required bandwidths of the optical analog links had to be determined. This information was inferred from the specifications and circuit diagrams of the sampling system used.[5,10] The bandwidth of the error link was determined by assuming the duration for which the memory gate opens (approximately 0.4 μs) to be twice the required rise time of the link. Thus using the formula, rise time $\times$ bandwidth $= 0.35$, a value of 1.8 MHz was obtained. The bandwidth of the feedback link was estimated from the maximum number of samples that can be obtained per second, and was found to be 43 kHz. The main requirement on the sampling command link is that it should introduce minimum time jitter into the sampling command signal.

The block diagram of the optically coupled sampling system is shown in Fig. 2. A brief description of the three fiber-optic links built for this project follows.

A. Fiber-optic error link

Figure 3 shows the fiber-optic error transmitter and receiver circuits that were constructed. The error link is built around a matched fiber-optic transmitter and receiver pair that was obtained commercially. The nominal bandwidth presented by this pair is 1 MHz.

R1 and R2 in the circuits of Fig. 3 set the input dc level at the center of the linear region of operation of the transmitter. The inverting amplifier at the output of the link serves to compensate for the phase reversal introduced by the fiber-optic receiver, along with providing a means to adjust the overall link gain to unity. This amplifier is built around a fast operational amplifier to minimize degradation to the overall link output rise time.

Tests on the error link showed that it has a bandwidth of 810 kHz. This bandwidth is about one half the nominal bandwidth of the original error circuits in the sampling system. Due to the nature of operation of the sampling system,[9] the limited bandwidth could be counteracted simply by com-

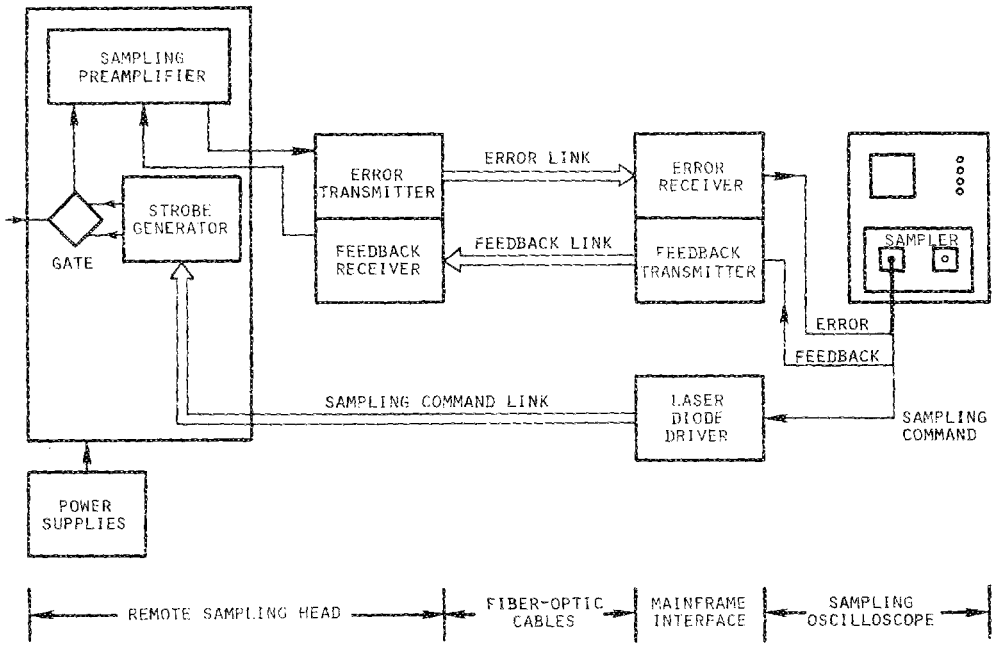

FIG. 2. Block diagram of the optically coupled sampling system implemented by the authors.

pensating for the delay in the error signal caused by the introduction of the fiber-optic error link. For this purpose, the adjustable memory gate width[10] in the sampling plug-in unit was increased to its maximum value (approximately twice its nominal value) to enable the memory circuit to capture the error signal before the gate closes. This necessary adjustment increases the noise allowed into the memory circuit during the opening time of the gate. The consequences of the additional noise are discussed in Sec. III.

B. Fiber-optic feedback link

The feedback link (Figs. 4 and 5) is dc coupled to facilitate transmission of the dc voltage injected into the feedback signal at the sampling plug-in unit.[9] The first stage in the feedback transmitter is an amplifier whose gain can be set to 5, 2, or 1, depending on whether the sampling signal is small, medium, or large in amplitude, respectively. This technique allows enhancing the signal-to-noise ratio (S/N) of the link for small- and medium-amplitude signals. In Fig. 5, the gain of the inverting amplifier circuit at the output of the fiber-optic feedback receiver can be set to $\frac{1}{5}$, $\frac{1}{2}$ or 1, to cancel the gain introduced at the transmitter. The last stage at the receiver provides a means for adjusting the dc level of the feedback signal delivered to the sampling head. Tests showed the feedback link to have a bandwidth of about 80 kHz, which is above the minimum value required for proper operation.

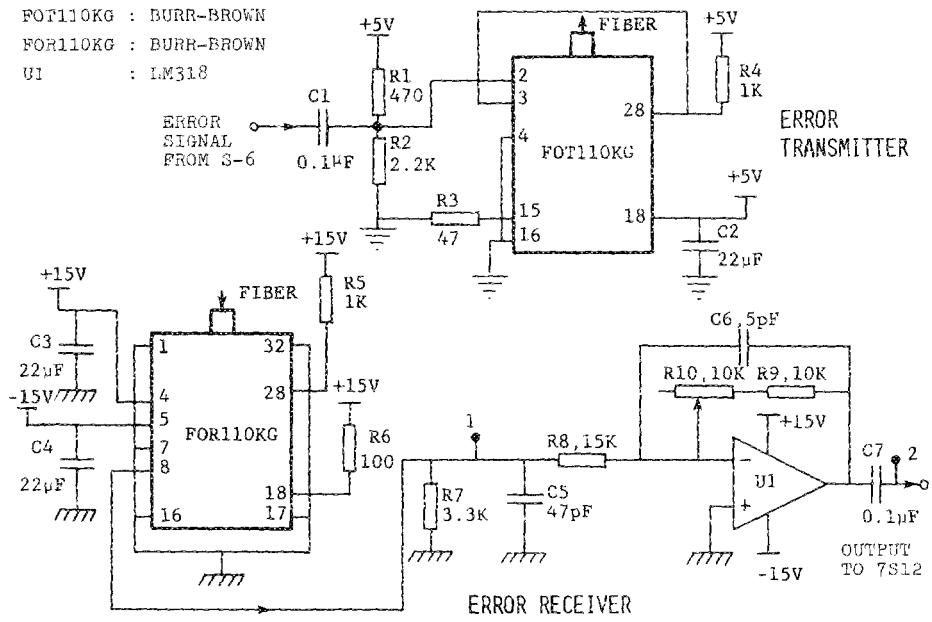

FIG. 3. Circuit diagram of the fiber-optic error transmitter and error receiver. The transmitting package (FOT110KG) and the receiving package (FOR110KG) were obtained commercially.

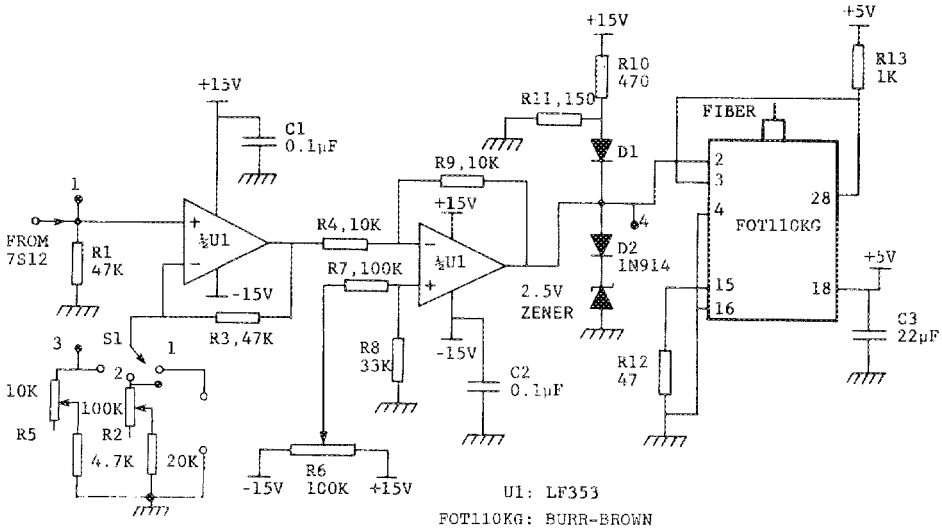

FIG. 4. Circuit diagram of the fiber-optic feedback transmitter. The transmitting package (FOT110KG) was obtained commercially.

C. Fiber-optic sampling command link

Figure 6 shows the circuit used to drive a high-power infrared gallium arsenide injection laser diode designed for pulsed operation. The diode was mated by the manufacturer to 20 ft of a high-quality glass fiber pigtail. The power launched into the fiber is 1.2 W when a maximum pulse current of 10 A flows through the diode. The circuit of Fig. 6 utilizes four transistors operated in the avalanche mode to generate a total estimated pulse current of about 6 A through the laser diode. The falling edge of the sampling command signal causes the four transistors to avalanche simultaneously. The charges stored in the small capacitors C1–C4 are dissipated through the collectors of the respective avalanche transistors, causing a current surge to pass through the laser diode LD. The current pulse can be observed with a wideband oscilloscope as a voltage drop across the monitoring resistance R_m. The current pulse was found to have a first transition duration of 1 ns.

At the sampling head, the infrared sampling command laser pulse is directly detected by the avalanche transistor (Q70, see schematic[5]) in the first stage of the strobe generator board. In the original (hardwired) sampling system configuration, this avalanche transistor is electrically triggered by the sampling command signal. The technique of triggering the avalanche transistor directly by the laser pulse[11,12] was implemented by shaving off the top of the metal cap on the transistor, then securing the end of the glass fiber to the top surface of the exposed transistor chip with the aid of a quick self-hardening epoxy (Fig. 7). The infrared radiation imparted into the transistor chip is powerful enough to penetrate the silicon chip and reach the reverse-biased collector-base junction. The infrared energy causes some electrons to be removed from the valance band into the conduction band, where they are accelerated by the high-intensity electric field in the reverse-biased junction, thus removing other electrons and eventually starting the avalanche breakdown. This detection technique eliminates the need for extra detection devices, and thus reduces the noise and consequently the time jitter introduced to the sampling command signal.

Figure 8 shows a photograph of the optically coupled sampling system. The remote part of the system was powered using four sets of rechargeable NICAD batteries.

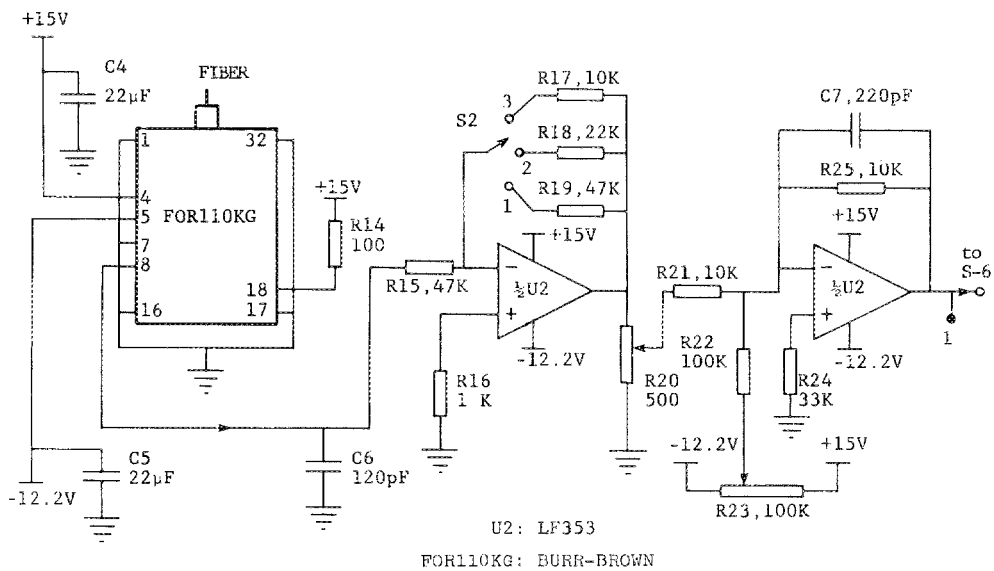

FIG. 5. Circuit diagram of the fiber-optic feedback receiver. The receiving package (FOR110KG) was obtained commercially.

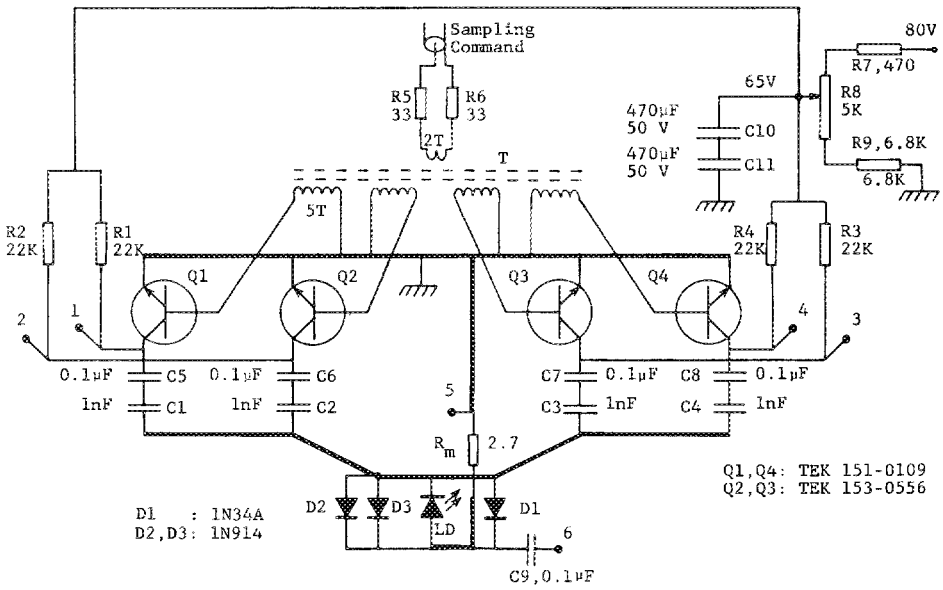

FIG. 6. Circuit diagram of the pulsed laser diode driver. When avalanche transistors Q1–Q4 receive a sampling command through the pulse transformer T, a current impulse of about 6 A passes through the laser diode LD.

The batteries supply the low voltages and power a dc–dc converter that is used to obtain the $+50$ and -50 V required by the sampling head.

III. SYSTEM PERFORMANCE

The tests conducted on the fiber-optically coupled sampling system fall into two categories: in the first, a visual or qualitative evaluation of system performance was sought; in the second, a quantitative evaluation was carried out. A step signal with a transition duration on the order of 100 ps and two different amplitude levels was used to conduct the tests. A large signal amplitude (approximately 270 mV) was required to characterize strobe jitter, along with distortions introduced by the analog links. A small test signal with an amplitude of approximately 15 mV was used to qualitatively characterize the noise behavior of the optically coupled system. In addition to testing the fully optically coupled sampling system, other tests were carried out with certain links being optically coupled while others were left hardwired. This approach was necessary to separately identify the factors affecting system performance. The system configurations tested are as follows:

(1) fully optically coupled sampling system (FOCSS): all links are fiber optic;

(2) laser strobed sampling system (LSSS): the sampling command is delivered by the laser link, while the error and feedback links are hardwired;

(3) error and feedback optically coupled sampling system (EFOCSS): error and feedback are fiber-optically coupled, while sampling command is hardwired.

In addition to the above three configurations, the normal (hardwired) sampling system was also used to acquire waveforms to serve as reference.

For the system configurations (1), (2), and (3) above, the memory gate was opened to its maximum width. Although this was not necessary for (2), it was done for the sake of uniformity. The transmitter-gain/receiver-attenuation ratio of the fiber-optic feedback link was set to 1/1 for large test signals, and 5/5 for small signals (see Sec. II). The "smoothing" function in the sampling system was turned off for all tests to avoid noise correlation between sequential samples.

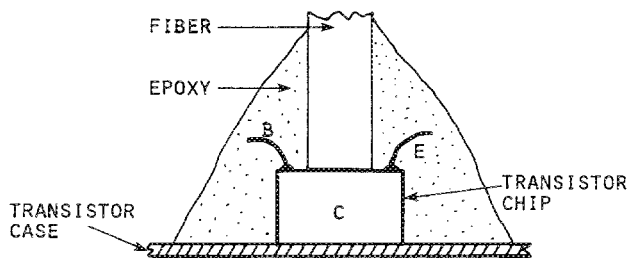

FIG. 7. Mating the glass fiber to the avalanche transistor chip.

A. Qualitative tests

Figure 9(a) shows a single acquisition of the leading edge of the large reference test signal acquired using the hardwired sampling system. Figures 9(b)–9(d) show the same waveform acquired by the three test configurations listed above. The strobe jitter introduced by the laser link is apparent on the rising edge of the waveform in Fig. 9(c). The jitter is nominal in the case of the waveform in Fig. 9(d), but the vertical noise level is seen to be higher than that of the reference waveform. The higher noise level is due to both the widely opened memory gate and the noise introduced by the analog links. The waveform in Fig. 9(b), acquired with the fully optically coupled system, shows the effects of both the superimposed noise and the strobe jitter. The spikes associated with strobe jitter are less pronounced here than those of the waveform in Fig. 9(c). The smoothing of jitter spikes is due to the lowpass nature of the error link.

Figure 10 shows the result of applying additive signal averaging[13] to 100 acquisitions of the waveforms of Fig. 9. The 10%–90% transition duration (T_r) indicated on the waveforms of Fig. 10 is a subjective parameter, and is measured between the points marked 1 and 2 . The transition duration of the waveform in Fig. 10(c) is longer than that of the reference waveform. The increased transition duration is

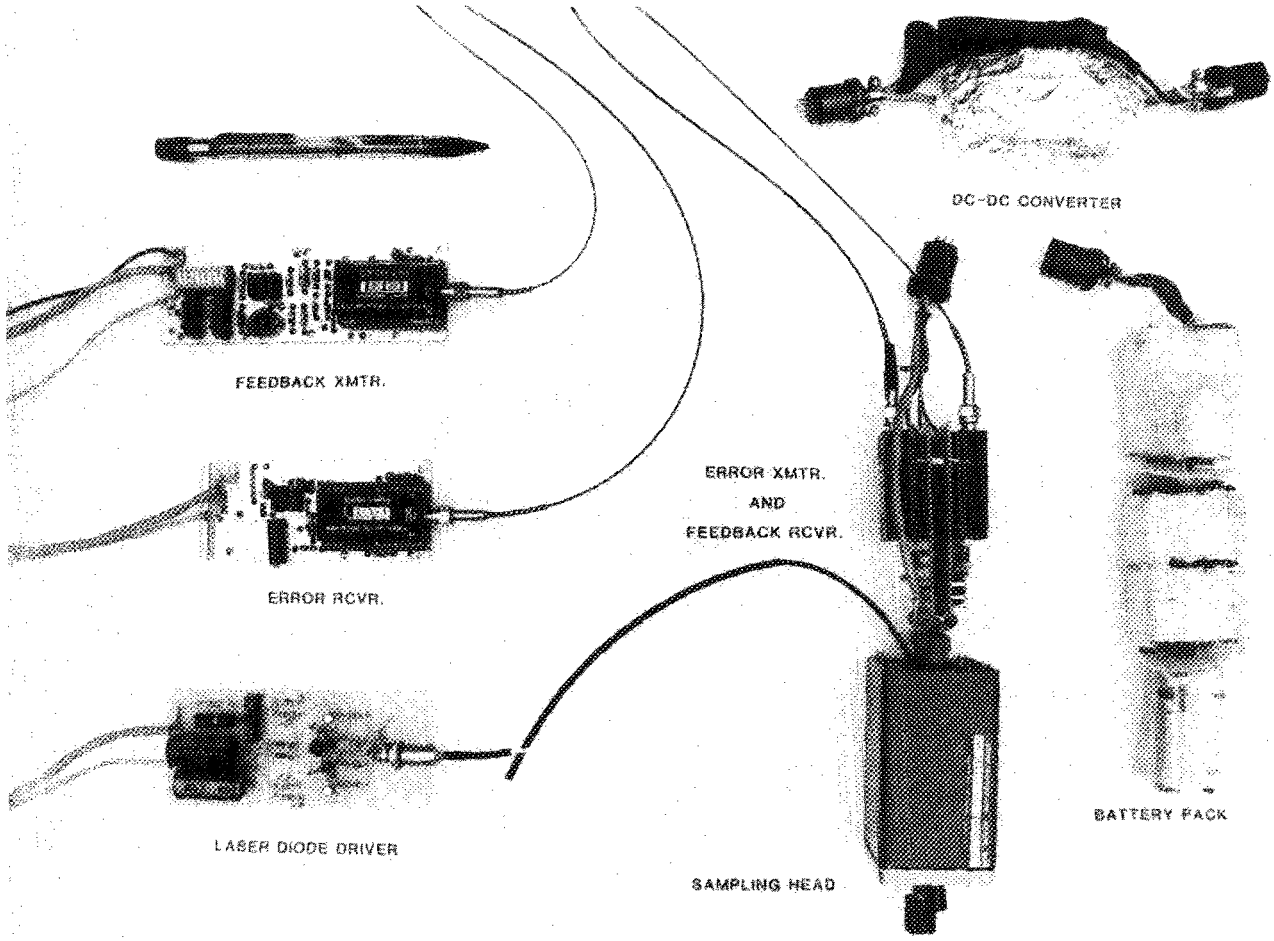

FIG. 8. Photograph of the fiber-optically coupled sampling system.

the first indication of the lowpass nature of the optically coupled sampling system, caused by the jitter introduced to the sampling command signal by the laser link.[14,15] The transition duration of the waveform in Fig. 10(d) is slightly higher than that of the reference, indicating a slight lowpass effect introduced by the analog links, mainly the error link.

Figure 11 illustrates the result of averaging 100 acquisitions of the leading edge of the small test signal. The vertical noise level in these waveforms is more evident than in the large-amplitude waveforms of Fig. 10. The transition durations of the different waveforms of Fig. 11 do not bear the same relationships to each other as those of Fig. 10, due to the error introduced into the transition duration measurement by the superimposed noise.

B. Quantitative tests

The aim of these tests was to find frequency-domain Fourier transform functions that characterize the performance of the fully (or partially) optically coupled sampling system configuration(s) relative to that of the standard (hardwired) system. Such transform functions were obtained simply by acquiring a signal using both the system configuration under study and the hardwired system, and then dividing the discrete Fourier transform (DFT) of the first waveform by that of the second.

The waveforms used to compute the transform functions were the result of additively averaging 100 acquisitions in a time window of 5 ns; they had 128 sample points and were steplike in nature, beginning and ending at different voltage levels. The direct transformation of such waveforms would yield erroneous transform functions due to the abrupt time-domain discontinuity at the end of the sampling window.[16] To circumvent this difficulty, pulselike waveforms were synthesized out of the steplike waveforms before transformation, using a method developed by Gans and Nahman.[16] The transform functions presented later in this section have a frequency resolution of 100 MHz. Although these functions are strictly defined only at a discrete set of frequencies, they will be shown as continuous functions for convenience.

Frequency-domain transform functions were obtained using large-amplitude test signals (approximately 270 mV) for the fully optically coupled sampling system (FOCSS) and the two other partially coupled system configurations (LSSS and EFOCSS). These functions are denoted by $S_F(f)$, $S_L(f)$, and $S_{EF}(f)$, respectively. Figure 12 shows the magnitude part of the three transform functions, while

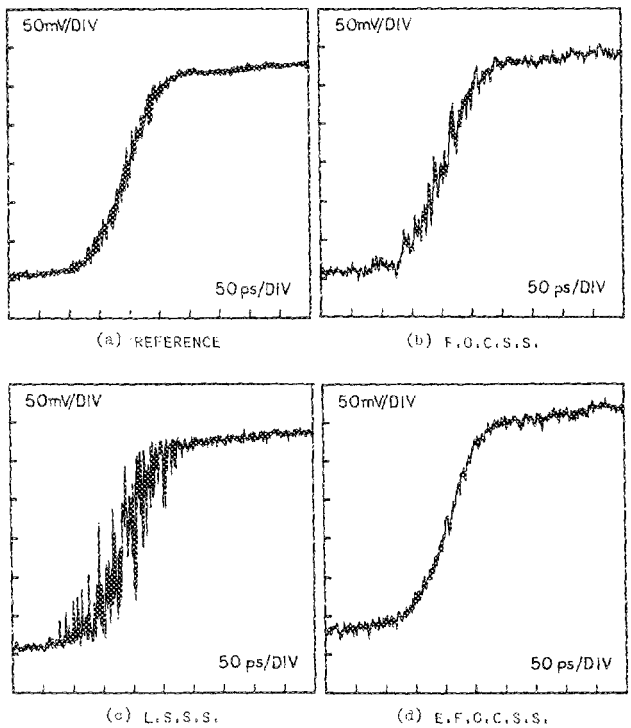

FIG. 9. Single acquisition of the leading edge of the large-signal test pulse: (a) hardwired (reference) system, (b) fully optically coupled sampling system, (c) laser strobed sampling system (error and feedback were hardwired), and (d) error and feedback coupled sampling system (sampling command was hardwired).

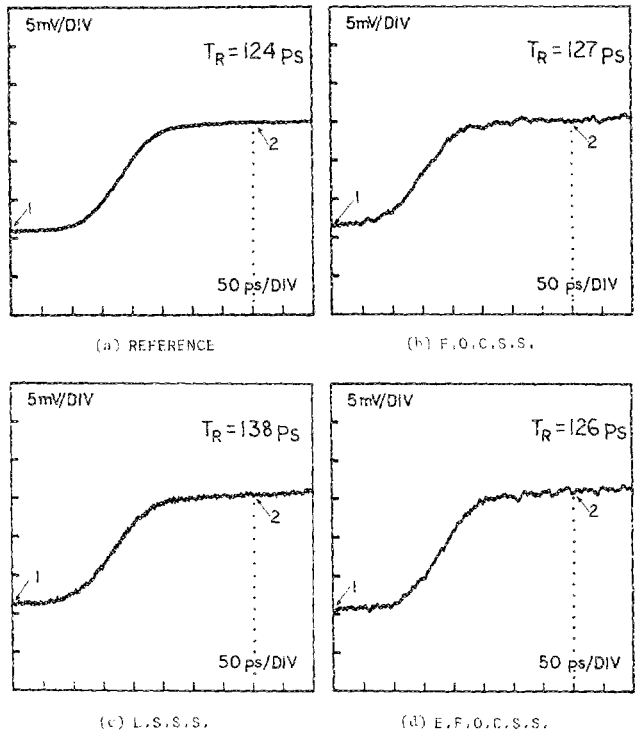

FIG. 11. The waveforms resulting from averaging 100 acquisitions of the leading edge of the small-signal test pulse: (a) hardwired (reference) system, (b) fully optically coupled sampling system, (c) laser strobed sampling system (error and feedback were hardwired), and (d) error and feedback coupled sampling system (sampling command was hardwired).

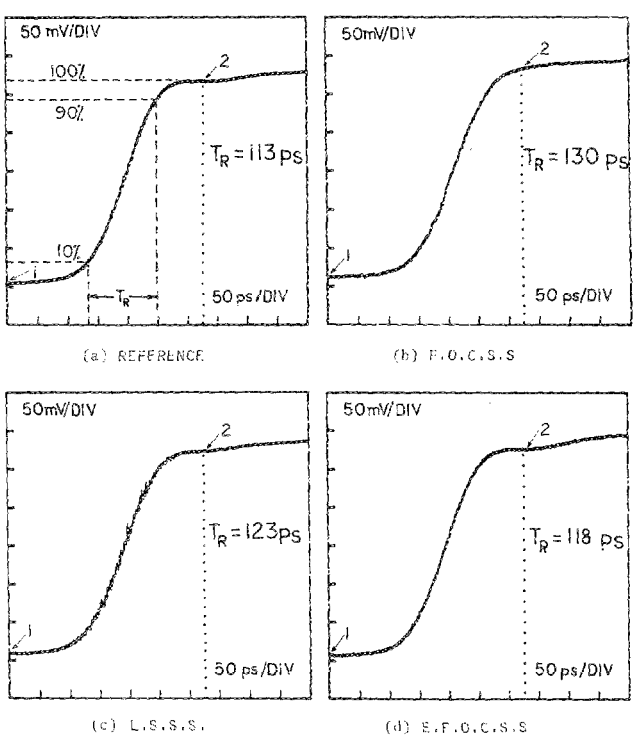

FIG. 10. The waveforms resulting from averaging 100 acquisitions of the leading edge of the large-signal test pulse of Fig. 9: (a) hardwired (reference) system, (b) fully optically coupled sampling system, (c) laser strobed sampling system (error and feedback were hardwired), and (d) error and feedback coupled sampling system (sampling command was hardwired).

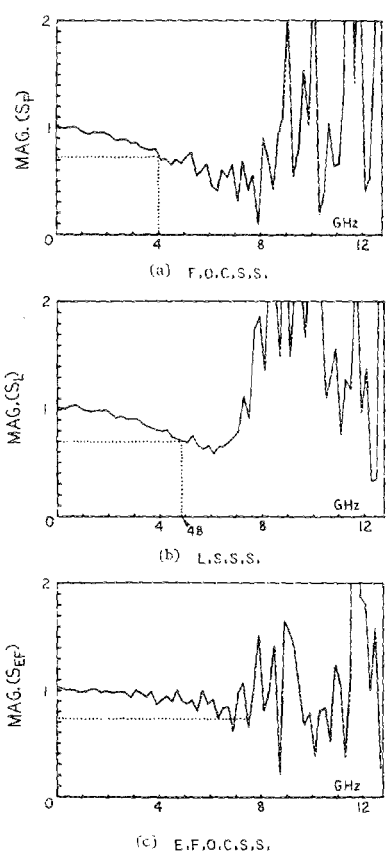

FIG. 12. The magnitude part of the transform functions $S_F(f)$, $S_L(f)$, and $S_{EF}(f)$. These functions characterize the three fiber-optic test system configurations relative to the hardwired system: (a) fully optically coupled sampling system, (b) laser strobed sampling system (error and feedback were hardwired), and (c) error and feedback coupled sampling system (sampling command was hardwired).

Fig. 13 shows the phase part of these functions. The lowpass nature of the sampling system due to the increased strobe jitter is evident in the magnitude part of $S_L(f)$. The magnitude part of $S_{EF}(f)$ is only slightly lowpass. The slight lowpass behavior of the latter function could be due to a sampling loop gain which is slightly less than unity.[17] The overall system bandwidth is seen to be 4 GHz, as measured at the 0.707 level of $S_F(f)$. Above a frequency of about 6 GHz, the spectra of the transform functions are dominated by noise.

The phase part of $S_F(f)$, $S_L(f)$, and $S_{EF}(f)$ is essentially zero except for a linear component of about 0°–20° in the range 0–6 GHz. The linear phase can be attributed to a slight displacement of the test waveforms in their time windows.

Transform functions were also obtained for the case of small test signals (approximately 15 mV) using the same procedure as for the large signals. The small-signal functions (not shown here) were noise corrupted due to the low signal-to-noise ratio of the small-amplitude test signals. One method of improving the S/N ratio of the small-signal test waveforms would have been to significantly average more than 100 acquisitions; this was not done, however, since the remote sampling head was operated with an unregulated rechargeable battery pack, and extended acquisition times would have resulted in excessive horizontal and vertical drift, distorting the resulting waveform averages.

IV. CONCLUSIONS AND RECOMMENDATIONS

The transform function $S_F(f)$ obtained in the previous section can be regarded as being essentially the transfer function of the optically coupled sampling system. This assertion is valid since the useful range of frequencies of $S_F(f)$ is well within the flat region of the response of the normal (hardwired) system, which is known to have a bandwidth of 11.5 GHz.[5] Thus the bandwidth of the optically coupled sampling system is that of $S_F(f)$, namely, 4 GHz. The lowpass behavior of the optically coupled system is due mainly to the strobe jitter introduced by the sampling command laser link. This can be seen from the lowpass nature of $S_F(f)$ and $S_L(f)$, while $S_{EF}(f)$ is only slightly lowpass (Fig. 12). The above conclusion is further supported by the fact that the phase of $S_F(f)$ and $S_L(f)$ is essentially zero, except for a linear component due to temporal waveform displacements. This zero phase shift, along with the Gaussian-like shape of the magnitude parts of $S_F(f)$ and $S_L(f)$ (in the frequency range of interest), is exactly what Gans[14] has predicted for a system where additive signal averaging is employed in the presence of strobe jitter. In his treatment, Gans has shown that when additive signal averaging is applied to an infinite number of acquisitions in the presence of normally distributed strobe jitter, the resulting effect is that of introducing to the sampling system a lowpass filter whose time-domain impulse response is a Gaussian function of the form

$$g(t) = K \exp[-0.5(t/\sigma_t)^2], \tag{1}$$

where K is a constant, and σ_t is the standard deviation of the jitter in the sampling strobe. The frequency-domain transfer function of this filter is

$$G(f) = C \exp[-0.5(f/\sigma_f)^2], \tag{2}$$

where $C = K\sigma_t\sqrt{2\pi}$ and $\sigma_f = 1/(2\pi\sigma_t)$. The previous equations were used to arrive at an estimate of the standard deviation of the sampling command jitter introduced by the laser link. Thus for the LSSS, which has a 3-dB bandwidth of 4.8 GHz, Eq. (2) gives, $\sigma_f = 5.76$ GHz. From this, the standard deviation of the introduced sampling command jitter is seen to be $\sigma_t = 28$ ps.

The vertical noise introduced to the waveforms acquired with the optically coupled system is due to two factors. The first is the widely opened memory gate, which admits more noise to the memory circuit. The second is the noise introduced to the error and feedback signals by the two analog links.

Improvements in the noise and bandwidth performance of the optically coupled sampling system can be achieved in a future version of the system that takes into account the following points.

(1) If a fiber-optic error link of limited bandwidth is used (in order to limit the noise bandwidth), then the memory gate generator in the 7S12 sampling unit must be modified to allow delaying the memory gate pulse by up to about 0.5 μs. This technique would eliminate the need for widely opening the memory gate, and thus reduce the noise superimposed on the acquired waveforms.

(2) Analog links with a maximum noise level of less than about 0.1 mV rms must be used to reduce the noise introduced to the error and feedback signals. Careful shielding and grounding of the links is recommended.

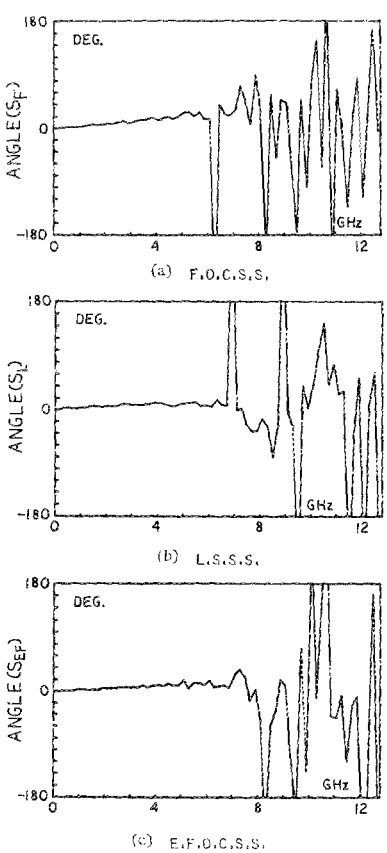

FIG. 13. The phase part of the transform functions $S_F(f)$, $S_L(f)$, and $S_{EF}(f)$. These functions characterize the three fiber-optic test system configurations relative to the hardwired system: (a) fully optically coupled sampling system, (b) laser strobed sampling system (error and feedback were hardwired), and (c) error and feedback coupled sampling system (sampling command was hardwired).

(3) Onboard voltage regulation must be added to the remote part of the system to avoid the drift caused by the drop of the voltage supplied by the rechargeable battery pack.

(4) A higher bandwidth than 4 GHz may be obtainable. If the present sampling command link is to be used, a reduction in strobe jitter may be achieved by increasing the current through the laser diode to its maximum allowable value, and/or experimenting with different avalanche transistors to be used for detecting the laser pulse in the strobe generator board of the sampling head. In addition to avalanche noise, the jitter in the sampling command is believed to be due to the scintillation of the optical intensity of the laser diode between consecutive pulses. The scintillation, which is on the order of a few percent, contributes to the jitter by varying the time that the detecting avalanche transistor needs to integrate enough infrared energy to avalanche. To minimize this effect, commercially available pulsed laser diodes whose optical output is more than 10 W may be employed.

AKNOWLEDGMENTS

This research was sponsored in part by the Office of Naval Research, contract No. N00014-81-K-0256. An abstract of this paper was presented at the URSI meeting held in Vancouver, British Columbia, Canada, June 1985. The authors wish to express their appreciation to Dean Allie M. Smith of the School of Engineering at the University of Mississippi for some of the financial support for this work. We are grateful to Dr. Mary Ryan-Hotchkiss, Ronald E. Correll, and Mihir Ravel of Tektronix Inc. for their help and useful suggestions. We also wish to thank Davis L. Dickerson and Raymond J. Cronin for the fabrication of some support electronics, and Dr. James G. Vaughan for his kind help.

[1]L. W. Pearson and Y. M. Lee, IEEE Trans. Antennas Propag. **AP-30**, 260 (1982).
[2]R. L. Holbrook, M.S. thesis, University of Kentucky, 1982.
[3]S. A. Dyer, R. L. Holbrook, and L. W. Pearson, Electromagnetics Research Report 82-3, University of Kentucky, 1982.
[4]S. A. Dyer and R. L. Holbrook, IEEE Trans. Instrum. Meas. (in press).
[5]Tektronix Inc., *S-6 Sampling Head, Instruction Manual* (Beaverton, OR, 1971).
[6]R. A. Lawton and J. R. Andrews, United States Patent 4,030,840, 21 June 1977.
[7]R. A. Lawton and J. R. Andrews, IEEE Trans. Instrum. Meas. **IM-25**, 56 (1976).
[8]J. R. Andrews and R. A. Lawton, Rev. Sci. Instrum. **47**, 311 (1976).
[9]Tektronix Inc., *Sampling Oscilloscope Circuits* (Beaverton, OR, 1970).
[10]Tektronix Inc., *7S12 TDR/Sampler, Instruction Manual* (Beaverton, OR, 1971).
[11]Dr. S. A. Dyer of Kansas State University has kindly brought the attention of the authors to this technique.
[12]S. W. Thomas and L. W. Coleman, Appl. Phys. Lett. **20**, 83 (1972).
[13]R. W. Ramirez, *The FFT Fundamentals and Concepts* (Prentice-Hall, Englewood Cliffs, NJ, 1985), p. 95.
[14]W. L. Gans, M.S. thesis, University of Colorado, 1975.
[15]W. L. Gans and J. R. Andrews, NBS Tech. Note 672, Sept. 1975, pp. 110–115.
[16]W. L. Gans and N. S. Nahman, IEEE Trans. Instrum. Meas. **IM-31**, 97 (1982).
[17]Tektronix Inc., *Sampling Oscilloscope Circuits* (Beaverton, OR, 1970), p. 16.